Rheo-NMR: a New Application for NMR Microscopy and NMR Spectroscopy

Paul T. Callaghan and **Elmar Fischer**, Institute of Fundamental Sciences-Physics, Massey University, Palmerston North, New Zealand

Introduction

Nuclear Magnetic Resonance is a remarkably powerful technique for the investigation of molecular structure, organisation and dynamics, and this fact lies behind the wide use of NMR in so many different fields of research in physics, chemistry, biochemistry, medicine, food technology and materials science. Chemical engineering is one of the areas that has more recently begun to benefit from the insights which NMR can offer, and two research topics where NMR is making a major impact are the study of flow in porous media and rheology, the study of the mechanical properties of complex fluids. The name derives from the Greek word "rheo" which means "to flow".

A detailed review of the science of Rheo-NMR has recently appeared [*1*]. Here we will outline the underlying principles and present a few examples which demonstrate how Rheo-NMR experiments can be carried out using a commercial NMR spectrometer. At the heart of the new method is the dual focus on NMR microscopy and NMR spectroscopy, the former giving insight at the mechanical length scale and the latter at the molecular length scale. For this reason Bruker spectrometers, with their powerful, multinuclear, microimaging capabilities, are ideally suited for Rheo-NMR studies.

Rheology

We tend to classify condensed matter as being in one of two basic phases: solid or liquid. When subjected to stress, a solid will deform by a fixed amount and store energy elastically. In contrast, a liquid flows and dissipates energy continuously as viscous losses. But in practice, many interesting materials in their condensed phase possess both solid and liquid-like properties. These include polymer melts and solutions, lyotropic and thermotropic liquid crystals, micellar surfactant phases, colloidal suspensions and emulsions. Most biological fluids, most food materials and many fluids important in industrial processing or engineering applications comprise elements of such complexity. Complex fluids exhibit both an elastic and a viscous response, i.e., both solid and liquid character. They possess "memory",

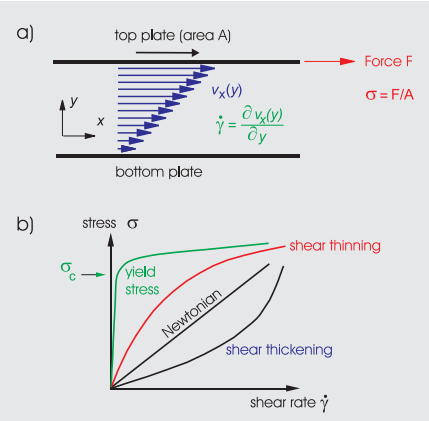

Fig. 1: ***a)*** *Velocity distribution in a Newtonian liquid between a static and a moving plate;* ***b)*** *flow curves for different classes of material.*

which means that the stress they exhibit at any moment will generally depend on their history of deformation. They exhibit non-linear mechanical behaviour, which means that their mechanical properties may change as the deformation increases, an effect generally attributed to molecular reorganisation. And they invariably possess a wide range of characteristic time scales, from the rapid (ps to ns) local Brownian motion of small molecules or molecular segments, to the very slow (ms to s) motions associated with the reorganisation or reorientation of large molecular assemblies or macromolecules.

The really important questions in rheology concern the molecular basis of complex mechanical properties [*2,3*]. A better understanding of this basis means that we can better design desirable fluidic properties, better process modern materials based on polymers and organised molecular states, better produce foods of the right texture, and better understand how nature works. For example, we can learn how synovial fluid protects our joints or how a spider can extrude a silk protein whose strength surpasses that of steel. In one of the newest applications of Rheo-NMR the link between molecular and mechanical behaviours is being investigated.

In classical rheological measurements a material is subject to deformation, and the *stress* $\sigma(t)$ is monitored as a function of the time-dependent *strain* $\gamma(t)$. An example of simple *shear deformation* is shown in **Fig. 1a**. In this report we shall be concerned with the large strain response, the so-called non-linear viscoelastic behaviour. For complex fluids this generally takes the form of a steady-state shearing flow, for which the stress is measured as a function of the *strain rate* $\dot{\gamma}$.

$$\dot{\gamma} = \partial\gamma / \partial t \qquad (1)$$

Fig. 1b shows examples of flow curves for different classes of materials: Newtonian, shear-thinning, shear-thickening, fluids exhibiting a yield stress, and fluids exhibiting a constitutive instability.

The investigation of non-linear viscoelasticity by Rheo-NMR requires that the deformational flow be created within the RF coil inside the NMR magnet. For this purpose we have developed a wide variety of shearing and extensional flow cells, all of which can be mounted in the standard Bruker (wide-bore) microimaging probehead. In order to make the link between classical rheology measurements and NMR, it is important that one of the key mechanical parameters be measured in situ. In our case this is the strain rate $\dot{\gamma}$. Whereas the stress within a material varies uniformly according to mechanical conservation laws, the strain rate may be very heterogeneous, a point which we shall demonstrate here. This fact motivated us to design our system around Bruker's microimaging capabilities, with which we are able to obtain velocity-encoded images at high spatial resolution. Thus, we are able to directly measure the local strain rate at all points within the shearing or extensional flow cell.

Rheometric Cells for the Bruker Microimaging System

All deformational flow devices are driven by a drive shaft inserted in the bore of the magnet and turned by a stepper-motor gearbox assembly mounted above the magnet bore (**Fig. 2**). The stepper motor is controlled from the Bruker spectrometer using a simple pulse sequence which provides the required TTL pulses for the drive unit. Rotation speeds in the range 0.08 to 4.74 Hz are available, and these yield the strain rate ranges shown in

Table 1. One of the advantages of using small deformation cells [*4*] in a microimaging system is that we are able to utilize quite small sample volumes and study expensive model materials. A second advantage is that the small cell dimensions give access to quite high strain rates. Because the cells are compatible with the standard Bruker micro-imaging probehead, it is possible to utilize the multinuclear capabilities of the rf coils and the temperature control features of the spectrometer system.

Fig. 2 also shows a standard shear device, the *cone-and-plate cell*, mounted in the Bruker probe. A clearer indication of the cell geometry can be seen in **Fig. 3** where an assembled 7° cone-and-plate cell and the parts of a 4° cone-and-plate cell are shown in more detail.

Two other systems can be used to produce purely extensional flow. In the *four-roll mill* this is accomplished by steady rotation of the quadrupole rollers, while the biaxial extension cell utilizes transient squeezing of material between the upper and lower cylinders [*5*]. Table 1 summarizes the dimensions of the cells, each of which is constructed from combinations of glass, Teflon and PEEK. The Couette cell inner cylinders are either smooth or finely crosshatched to inhibit slip, and each has the capability of incorporating a marker fluid so that the rigid body motion of the inner cylinder can be imaged in order to determine, by extrapolation, the velocity of the cylinder surface.

Flow Visualisation of Heterogeneous Shear and Extension

The method we use to obtain velocity maps is quite standard [*6*] and relies on the insertion of an additional pair of gradient pulses to a standard spin-warp imaging sequence, as shown in the pulse sequence of **Fig. 4**. These so-called q gradient pulses (duration δ, separation Δ, and gradient strength g) result in a phase shift of the echo signal as a function of displacement of spins over the time interval Δ. Thus, the signal for each voxel corresponding to a pixel in the reconstructed image has a phase modulation factor Φ defined as

$$\Phi = \int \bar{P}_s(Z,\Delta)\exp(i2\pi qZ)\,dZ \quad (2)$$

$$q = \gamma g\delta/2\pi \quad (3)$$

where Z is the *spin displacement* along the gradient direction, q is the *reciprocal space vector*, is $\bar{P}_s(Z,\Delta)$ the *average propagator* (the probability that a spin-bearing molecule will move by a displacement Z in the time Δ), and the integral is taken over the voxel volume. Typically we acquire 8 separate 2D spatial images with different q amplitudes in about 15 to 30 min. A three-dimensional array is created with q as the third dimension, and Fourier transformation in the q dimension returns the propagator for each pixel. This propagator is a convolution of those resulting from dispersion (D) and mean flow alone so that its width is $(2D\Delta)^{1/2}$ while its displacement along the Z-axis is $v\Delta$, where v is the velocity component along that axis. Our image analysis software is used to obtain these parameters directly so that dispersion and velocity maps can be constructed automatically.

One of the most important shearing geometries used in the rheological characterization of fluids is that of the cone-and-plate cell. This device exhibits an almost uniform stress across the fluid contained in the gap, varying only as $\csc^2\theta$, where θ is the angle to the polar axis (e.g., for a 4° gap the variation is only 0.25%). Because the stress is approximately constant across the fluid, it is possible to use the cone-and-plate rheometer to step through the flow curve, point by point, obtaining corresponding σ and $\dot{\gamma}$ measurements. Regardless of whether a fluid is shear-thinning or shear-thickening, if slip effects are absent, the shear rate across the gap should be uniquely defined and identically equal to the rate determined by the external surfaces, $\omega/\tan\alpha$, where ω is the cone rotation rate. Thus, the cone-and-plate is the most popular device used to study non-linear viscosity in complex fluids.

In fact, NMR flow visualisation shows that the fundamental assumption of shear rate constancy is not valid for certain classes of fluid. **Fig. 5** shows two such examples of the velocity image and shear rate profile (a) across a wormlike micelle solution (100 mM cetylpyridinium chloride, 60 mM sodium salicylate) [*7*] and (b) in a commercial tomato sauce [*8*]. Both systems exhibit a phenom-

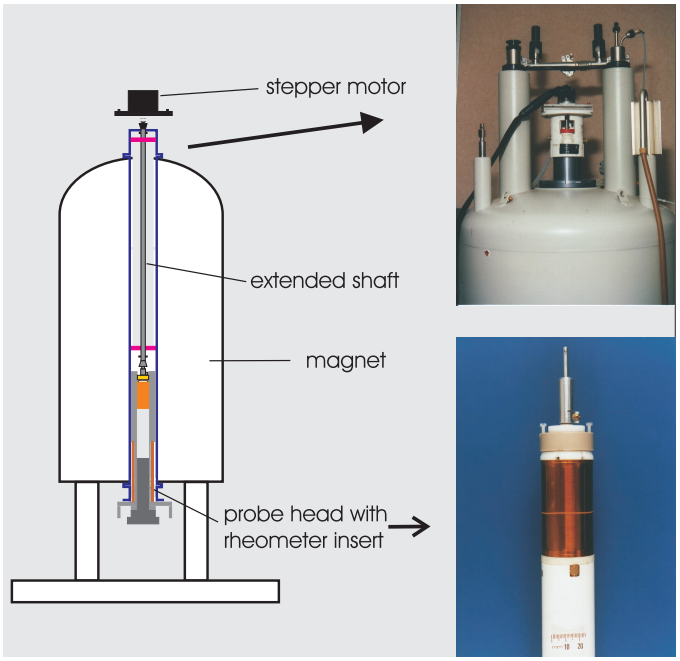

Fig. 2: *A standard superconducting wide-bore magnet is shown with motor, driving shaft, rheometric device and Bruker microimaging probehead.*

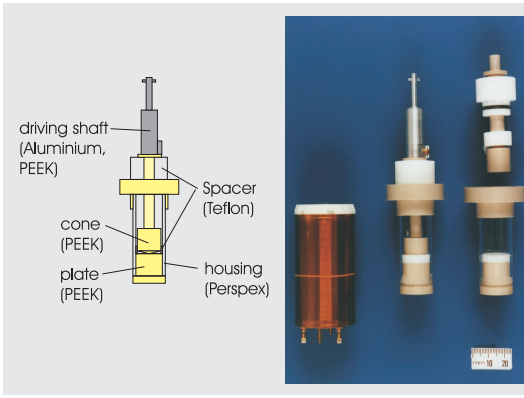

Fig. 3: *Cross section schematic and photo of the cone-and-plate rheometric cell.*

Table 1. *Characteristics of Rheometric Cells for NMR Microimaging.*

Rheometer Type	Dimensions [a] (mm)	Material	Shear Rate (s^{-1}) at 4.74 Hz rotation rate
Cone-and-plate	cone diam.: 24 or 16 angle: 4° or 7°	machinable glass (smooth)	426
PEEK Couette cell	ID: 19 OD: 17	PEEK (smooth or hatched)	253
PEEK Couette cell	ID: 19 OD: 18	PEEK (smooth or hatched)	536
Glass Couette cell	ID: 7.0 OD: 4.0	smooth glass cylinder, Teflon bushes	40
Glass Couette cell	ID: 9.0 OD: 7.5 or 5.0	smooth glass cylinder, Teflon bushes	149 or 37

[a]ID: inner diam. of chamber; OD: outer diam. of rotor.

enon known as shear banding, in which the fluid apparently separates into coexisting phases of widely differing viscosity. In the case of the wormlike micelle system, the NMR studies [*9,10*] have provided important new evidence for shear banding in a variety of geometries and have shed new light on flow instability and molecular ordering effects in these materials. These results show the vital contribution of Rheo-NMR studies to any understanding of flow curve behaviour in such materials where classical assumptions fail and where flow visualisation is essential. The ability of NMR to provide this essential information in an opaque material is an advantage of considerable importance.

Fig. 5b illustrates another nice feature of Rheo-NMR velocimetry when the same tomato sauce sample is viewed under shear in a cylindrical Couette cell. Extrapolation from the inner cylinder marker fluid shows that the sauce slips at the inner surface, has a variable shear across the annulus, and finally exhibits low slip at the outer surface. However the shear rate behaviour across the annulus exhibits significant heterogeneity [*8*]. A transition in shear rate is observed within the annulus, the velocity first decreasing and then increasing with radius in a manner similar to plug flow. However the inner (high stress) band is shear-thinning while the outer is plug-like. The separation into separate shear-thinning and plug-like phases represents a behaviour characteristic of yield stress properties, a feature which corresponds nicely with the observed macroscopic properties.

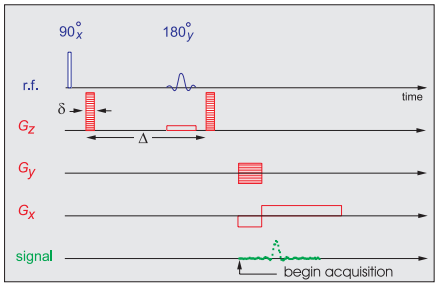

Fig. 4: *Spin-warp imaging sequence used for velocimetry.*

Finally, we show in **Fig. 6** the velocity map within the four-roll mill, in which pure planar extensional flow exists near the stagnant point at the cell center [*4*]. Selective excitation methods can be used to produce an NMR signal only from the central region of the cell, and this device makes it possible to carry out NMR spectroscopy on molecules subject to transient extensional strain as they are swept through this region of the flow.

Molecular Properties: Dynamics, Order and Alignment

Through the use of spectroscopic approaches Rheo-NMR holds the promise of linking mechanical and molecular properties. Amongst the spectroscopic tools which lend themselves to such studies are (i) the measurement of spin relaxation times to gain information about molecular rotational dynamics, (ii) the measurement of molecular diffusion coefficients in order to probe molecular organisation and (iii) the measurement of ^{1}H dipolar interactions, ^{13}C chemical shift anisotropy, or ^{2}H quadrupolar interactions in order to gain information about molecular alignment. Several examples of these approaches are given in [*1*], and we present two more recent applications here.

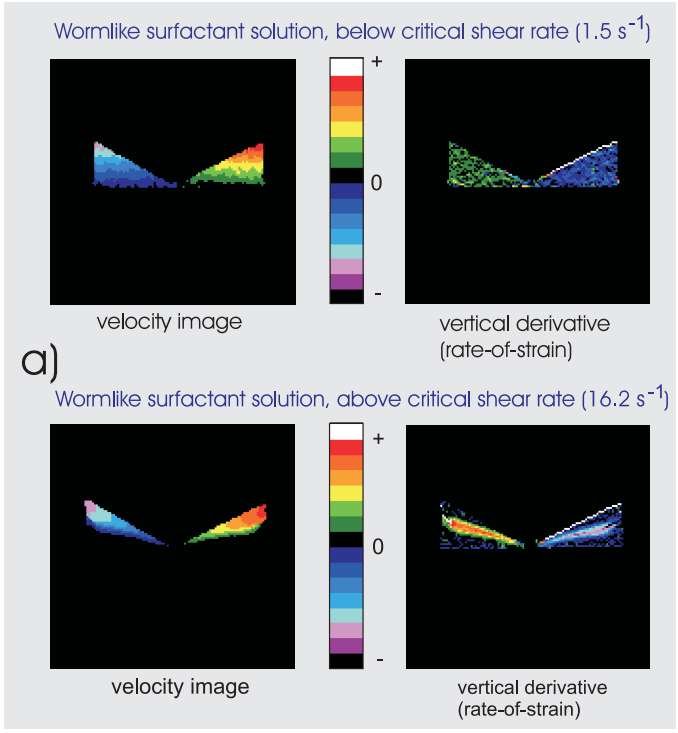

Fig. 5: ***a)*** *Velocity and shear rate profile across the gap for a wormlike surfactant solution below and above the critical shear rate.* ***b)*** *Velocity profile across the gap of a Couette rheometer for different types of tomato sauce, in which shear rate heterogeneity and yield stress effects are apparent. The one-dimensional velocity profile is taken from the region indicated by the white line.*

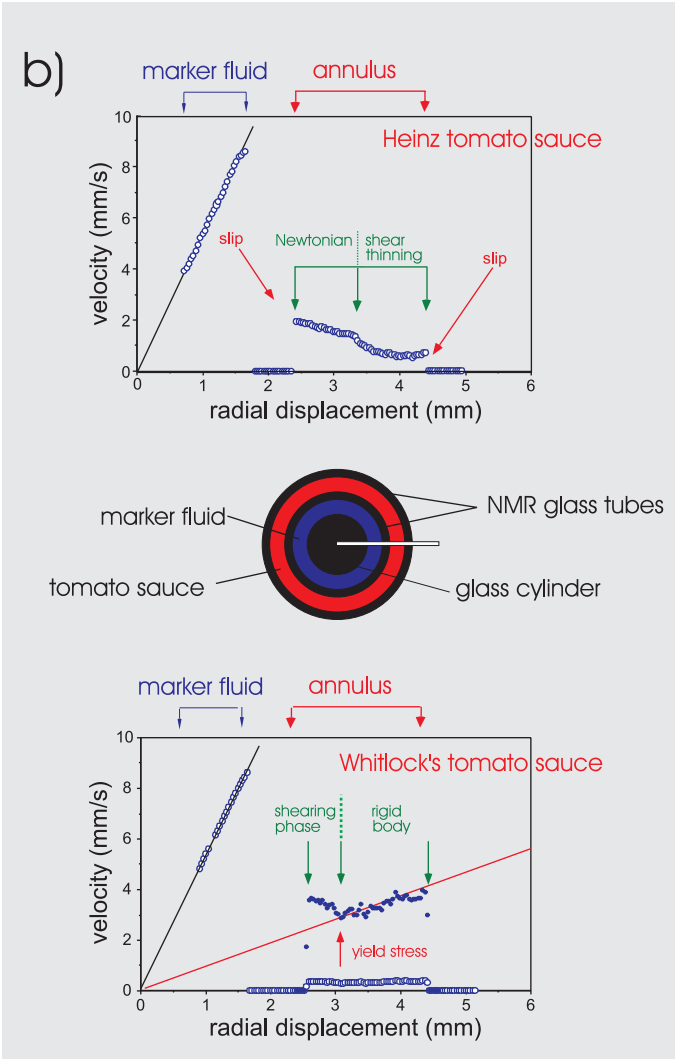

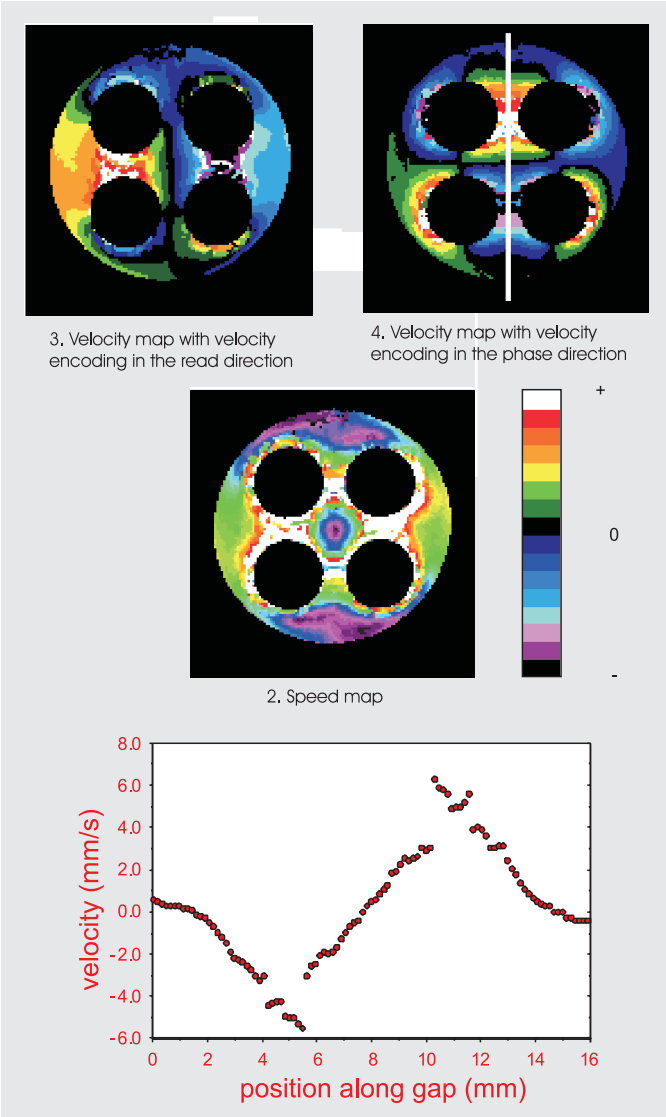

Fig. 6: *Velocity images for 3900-dalton polydimethylsiloxane melt under flow in the four-roll mill. The diagram at the bottom shows the dependence of velocity on position along a column through the center of the cell. The one-dimensional velocity profile is taken from the region indicated by the white line.*

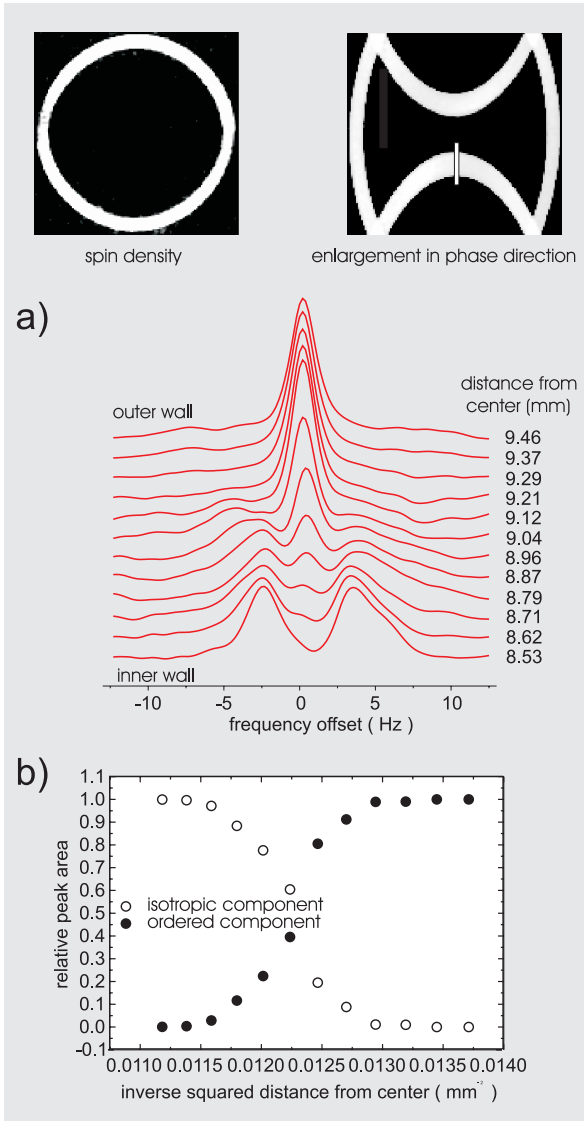

Fig. 7: *Solution of 18% cetyltrimethylammonium bromide in D_2O (40°C) in the 17-mm/19-mm Couette cell with enlargement of area of interest. The one dimensional velocity profile is taken from the region indicated by the white line. The average shear rate is 20 s^{-1}.* ***a)*** *^2H NMR spectra obtained at different positions across the gap.* ***b)*** *Relative peak areas of spectral components.*

An example of the use of quadrupole interaction spectroscopy is shown in **Fig. 7**, where the shear-induced order in the wormlike micelle solution (18% CTAB/D_2O at 40 °C) is investigated [*9*]. The ^{2}H-NMR spectrum of the D_2O is plotted as a function of radial position across the gap of a cylindrical Couette cell. At the inner wall, where the stress is highest, a splitting is observed, indicative of a finite quadrupole interaction, while at the outer wall a single peak is observed. These data suggest the formation of a nematic phase at high stress with a transition through a mixed phase region to an isotropic phase at the region of low stress. What is particularly interesting about this experiment is that the associated velocity profile shows a banding in the shear rate which does not correlate simply with the local order parameters reflected in the ^{2}H-NMR spectra. This indicates that the molecular ordering is associated with the monotonically varying stress, rather than the discontinuously varying rate of strain. The example provides valuable new insight regarding the origin of shear banding in systems close to an isotropic/nematic phase transition.

Another intriguing correlation between shearing and molecular conformation is shown in **Fig. 8**. Here the comparison is between the velocity profile and the local spin-spin relaxation time of protons in polyacrylamide in D_2O. In this case [*10*] the shear band structure correlates well with the T_2 map, with the region of high shear rate exhibiting a strongly enhanced rate of relaxation. This effect has been attributed to deformation of the polymer "entanglement tube" in the flow, such that the correlation time for segmental reorientation is lengthened. In contrast with the example shown in Fig. 7, no nematic/isotropic transition can be invoked for the case of polyacrylamide in water. It is believed that the shear banding arises from a constitutive instability in which the underlying stress vs. shear rate of the material exhibits a region of negative $\partial\sigma/\partial\dot{\gamma}$. The inset shows the recovery of T_2 when shearing stops; the time constant is then similar to the polymer terminal relaxation time, as measured by mechanical means. Again the combination of spatially resolved NMR spectroscopy and NMR velocimetry provides an opportunity to investigate local molecular interactions and their role in determining molecular properties.

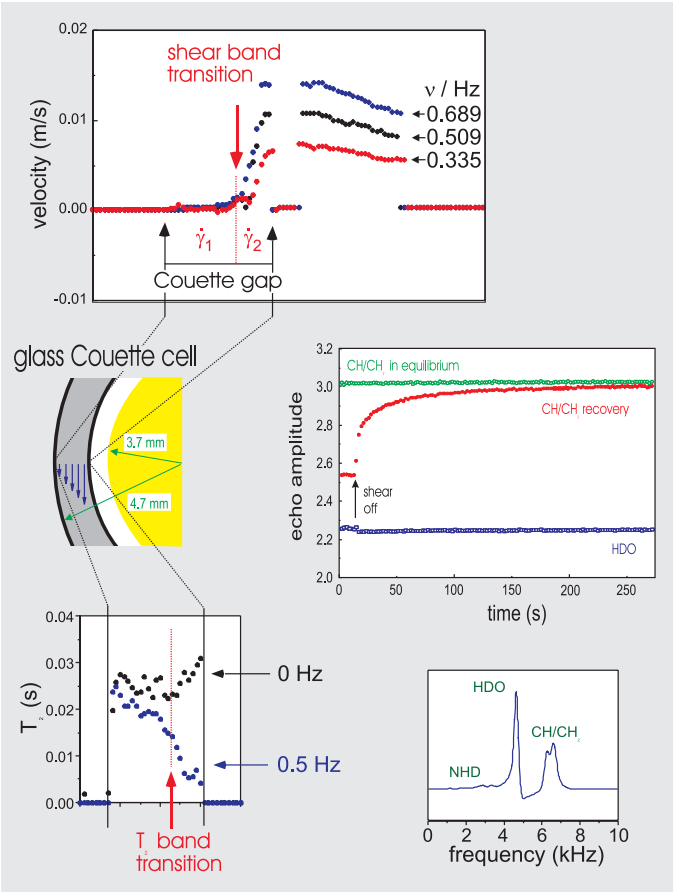

Fig. 8: *Velocity and T_2 profiles for a 3.0% solution of polyacrylamide (MW = 10^7 dalton) in D_2O under shear in the 7.5/9-mm Couette cell. Note the appearance of a shear band which corresponds with a band in T_2. The inset shows the transient recovery of T_2 following shear cessation.*

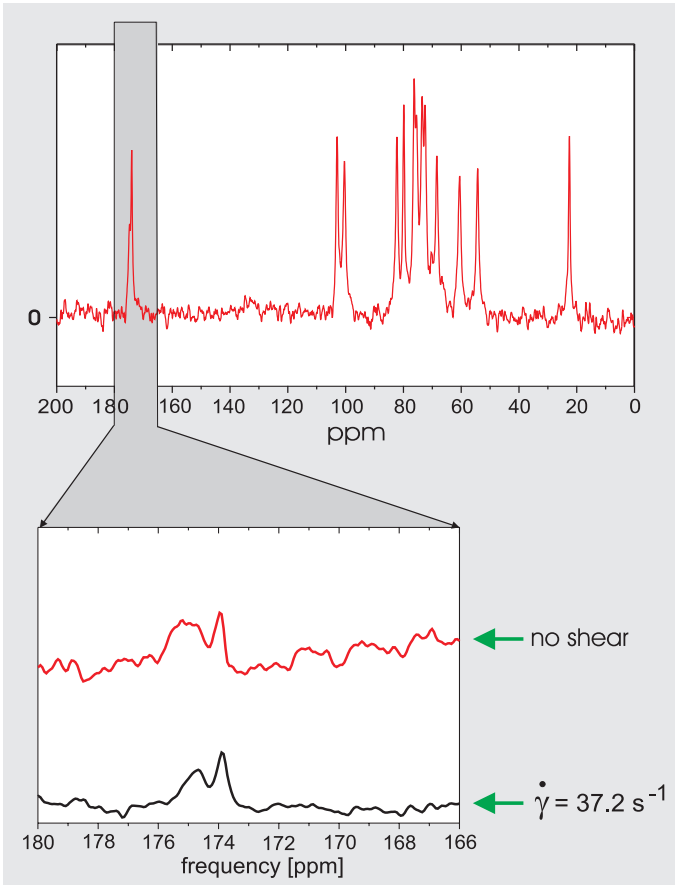

Fig. 9: *^{13}C spectra of 1% hyaluronan in D_2O buffer solution with and without shear (900 000 transients each). Note the small perturbation to the acetamido carbonyl peak.*

Modulation of Intermolecular Interactions

Central to an understanding of the tertiary structure of biological macromolecules is the role of intermolecular interactions such as hydrogen bonds. Under shearing flow, molecules on differing local streamlines are separated at a scale-independent rate given by $\dot{\gamma}$. If this rate (up to ca. 500 s^{-1} in our cells) exceeds the characteristic rate at which intermolecular bonds are naturally broken and reformed, then the tertiary structure is disrupted, and the moieties responsible for bond formation will exhibit quite different dynamics compared to the bonded state. Thus, Rheo-NMR provides a means of determining which sites on a molecule are responsible for intermolecular binding by simply comparing high-resolution NMR spectra obtained in states of equilibrium and under shear. An example is shown in **Fig. 9** where we compare two ^{13}C-NMR spectra (shear rate 0 s^{-1} vs. 37.2 s^{-1}) from hyaluronan, a polysaccharide in the synovial fluid [*10*]. The effect of shear on the NMR signal can be seen for the acetamido carbonyl, a moiety which is believed to be responsible for intermolecular hydrogen bonding.

Conclusions

The last example highlights the very general capabilities of the Rheo-NMR method. With the exception of the loss of sample space due to the presence of the central cylinder, there is no sacrifice in signal-to-noise ratio when NMR is performed under a shearing flow. The use of the cylindrical Couette cell, with all its machined faces (within the rf coil) oriented parallel to the B_0 field means that high spectral resolution can be achieved. Consequently, nearly all forms of NMR spectroscopy that are possible in equilibrium are also possible under shear. This opens the way for a wide range of NMR studies in which molecular sites responsible for intermolecular interactions can be identified and their reaction dynamics determined.

References

[*1*] P. T. Callaghan, Rheo-NMR: nuclear magnetic resonance and the rheology of complex fluids. *Reports on Progress in Physics* **62**, 599-670 (1999).

[*2*] R.B. Bird, R.C. Armstrong, O. Hassager, *Dynamics of Polymeric Liquids*, John Wiley & Sons, New York (1987).

[*3*] T.C.B. McLeish, *Theoretical Challenges in the Dynamics of Complex Fluids*, Kluwer, Dordrecht (1997).

[*4*] M.M. Britton, P.T. Callaghan, M.L. Kilfoil, E.W. Mair, K.M. Owens, NMR velocimetry and spectroscopy at microscopic resolution in small rheometric devices, *Appl. Magn. Reson.* **15**, 287-301 (1998).

[*5*] P.T. Callaghan, A.M. Gil, ^1H NMR spectroscopy of polymers under shear and extensional flow, *Rheo Acta* **38**, 528 - 536 (1999).

[*6*] P.T. Callaghan, *Principles of Nuclear Magnetic Resonance Microscopy*, Oxford (1991).

[*7*] M.M. Britton, P.T. Callaghan, Two-phase shear band structures at uniform stress, *Phys. Rev. Lett.* **78**, 4930-4933 (1997).

[*8*] M.M. Britton, P.T. Callaghan, NMR microscopy and the non-linear rheology of food materials, *Magn. Reson. Chem.* **35**, 37-46 (1997).

[*9*] E. Fischer, P.T. Callaghan, Is a birefringence band a shear band?, *Europhysics* **50**, 803-809 (2000)

[*10*] P.T. Callaghan, A.M. Gil, Rheo-NMR of semi-dilute polyacrylamide in water, *Macromolecules* **33**, 4116-4124 (2000).